Probabilistic Safety Evaluation of Geopolymer Concrete One Way Slabs Reinforced with GFRP Rebars

Sai Kumar. A[1], Kumaran. G[2]
[1]*Ph.D Scholar, Department of Civil & Structural Engg, Annamalai University.*
[2]*Professor, Department of Civil & Structural Engg, Annamalai University.*

***Abstract*—The unpredictability of factors affecting the flexural strength of structural elements is taken into consideration by reliability analysis. The development of structural dependability techniques offers a more stable foundation for the design codes to grow. The dependability analysis of the flexural behaviour of GFRP-GPC (Glass Fibre Reinforced polymer-Geo polymer Concrete) one way slabs is the main emphasis of this study. The uncertainties associated with modelling and statistics are part of the analysis. Models to describe variation in the existing structural materials and the structural loading are drawn from the literature. The dependability index is used to quantify structural reliability. For the flexural limit states, the changes in the reliability index with design loads are examined. The reliability has been evaluated using simulation and first-order reliability methods. It is also examined how the sectional dimensions and reinforcement ratio affect the dependability index. The results of this work bring to light the many variables affecting the reliability of GPC one way slabs reinforced with GFRP reinforcements and the need for continuing research to better describe these variables.**

***Index Terms*— Flexural strength, GFRP, GPC, One way slabs, Reliability.**

I. INTRODUCTION

The production of Portland cement contributes significantly to CO_2 emissions and resource depletion, strategies to reduce the environmental and sustainability issues that have emerged as a result of the widespread usage of Portland cement. Even though it is now impossible to completely eradicate Portland cement, efforts are being made to reduce its usage in concrete through ongoing technological advancements and the integration of cutting-edge technology. Many researches are currently being conducted to determine whether pozzolanic materials, such as fly ash, slag, rice husk ash, Metakolin, etc., can be used in place of cement entirely or in part when making concrete. Research is being conducted globally to develop materials and processes that use less energy and emit fewer pollutants; examples include changing the cement manufacturing process and creating substitute materials that are suitable. Similarly, because of their high tensile strength and good resistance to corrosion, Glass Fiber Reinforced Polymer (GFRP) rods can be a great substitute for traditional reinforcing bars. Rapid advancements in the study and use of these materials in civil infrastructures have led to the establishment of certain design criteria [1]-[8]. It is well known that FRP rods have lower moduli of elasticity than reinforcing bars. This is particularly true for GFRP rods, whose modulus of elasticity is just 20% to 25% of that of reinforcing bars. Even if the stress level in the concrete beam is not high, the low modulus of elasticity of the FRP rod would cause significant deflection. The dependability evaluation of the flexural capacity design of FRP reinforced structural members has recently received attention. Establishing a probability based design Technique for FRP reinforced concrete structures has become imperative due to fast advancement in the field applications of FRP in engineering structures. Some design standards have been created accordingly so far. According to these standards, the majority of the reduction factors related to FRP materials have been empirically altered from their counterparts in the design rules for RC structures. The mechanical and physical characteristics of FRP materials are very different from those of reinforcing bars. The strength ultimate state and the serviceability ultimate state are two examples of the extreme contrasts that result from these distinctions. It is unclear how the empirical reduction variables affect the degree of reliability. Even though the majority of FRP material data is still proprietary to manufacturers and there are currently few comparable test results for FRP strengthened concrete beams, a thorough evaluation of those reduction factors from a probabilistic perspective is still crucial because the evaluation would highlight some issues. This paper's primary goal is to provide a reliability assessment of the design specifications for GPC one way slabs reinforced with GFRP.

II. RELIABILITY ANALYSIS

In structural performance, "reliability" refers to the likelihood that the structure will carry out its intended function for the course of its anticipated lifetime in the given environmental conditions. The probability of failure P_f provides an alternative and complementary measure of reliability. Thus, a probability of failure of 0.001 is synonymous with a reliability of 99.9%. For structural elements, P_f is only an indicative measure and not an absolute measure of failure. Safety margins are applied to structures built using conventional techniques in order to reduce the possibility of failure. Therefore, the goal of reliability based design has been to rationally address the issue of "sufficient safety." The loads and material properties are the primary variables in design calculations that are exposed to different levels of randomness and uncertainty [9]-[27]. Due to the inherent unpredictability in the different design factors and the numerous uncertainties affecting the theoretical models, a probabilistic framework is required. Therefore, statistical and probabilistic analysis must serve as the foundation for a realistic, logical, and quantitative portrayal of safety.

III. OBJECTIVES

1. Determination of basic properties of the constituents of GPC and GFRP rebars experimentally.
2. Determination of Flexural performance of the GFRP - GPC slabs under two point static loading.
3. Theoretical Formulation of the Flexural performance of the GFRP - GPC slabs.
4. Determination of uncertainties involved in the Properties of materials, manufacturing methods of materials, Flexural performance of one way slabs that has been determined both experimentally and theoretically.
5. Determination of Reliability index and Resistance factor using FORM (First - Order Reliability Method).

IV. EXPERIMENTAL PROGRAMME

A. *Mix Proportions*

In this study, for preparing GPC mixes, the alkaline activator solutions are made by keeping concentration of sodium hydroxide solution as 12 M for M25 grade concrete and 14 M for M50 respectively. The mixer of sodium hydroxide (NaOH) solution with sodium silicate solution (Na_2SiO_3) at normal room temperature creates polymerization process with larger amount of heat. This mixer is kept for about 24 hours, to get the alkaline solution which now acts as a binding agent. Fly ash, GGBS and aggregates which have been taken according to the mix ration are then mixed in dry condition together for 2 minutes. The maximum percentage of GGBS is restricted to 30 % to get workable mix. The mixing ratio adopted for Geopolymer concrete, with fly ash and Alkali-Activator solution for 12M & 14M are tried in this study, along with Alkaline - Activator /fly ash ratios of 0.3 and 0.45. Based on the different trial studies, it is confirmed that the percentage of FA & GGBS in various molarities, 12M and 14M satisfies the M25 and M50 target strength respectively and it gives the optimum target strength values and are tabulated in Table I. Similarly, the tensile strength of the GFRP reinforcement used in the present study has been presented in Table II.

Table. I Mix proportions of GPC (M25)

INGREDIENTS	MIX	
	M25	M50
Molarity	12	14
Flyash (kg/m^3)	380.29	347.62
GGBS (kg/m^3)	42.25	283.81
NaOH (kg/m^3)	54.33	30.1
Na_2SiO_3 (kg/m^3)	135.8	134
Fine Aggregates (kg/m^3)	709.87	568.57
Coarse Aggregates (kg/m^3)	1267.62	1200
Water (kg/m^3)	32.60	23.8
SP (kg/m^3)	4.23	7.62
AAS/Binder	0.45	0.30
Mix Ratio	1:1.68:3	1:0.9:1.9
Workability (Slump, mm)	125	100

Table. II Tensile properties of reinforcements (Experiment)

Specimen ID	Peak Tensile load [kN]	Peak Tensile Extension [mm]	Ultimate Tensile Strength	Modulus of elasticity [MPa]

			[MPa]	
GFRP (Sample 1)	78.24	15.5	996.8	61651.74
GFRP (Sample 1)	78.35	16.2	998.1	61587.5
GFRP (Sample 1)	78.6	15.3	1001.2	65509.09

B. Test setup and Instrumentation (Static Loading)

The slab specimens are tested using a load frame with a 50Ton capacity. The end conditions for slabs are as follows: one end of the slab rests on a roller, while the other end rests on a hinge. Spreader beams are utilized in a two point loading (line loads) system. To prevent local effects, thick neoprene or rubber cushions are placed beneath the spreader beams. Spirit levels were used to maintain the slabs' support end levels. Hydraulic jacks with a 250 kN capacity are used to manually apply the static loads, and load cells or proving rings are used for monitoring. Dial gauges, surface strain pellets, LVDTs, and Demec gauges are used to measure the slab's deflections or deformations. External surface strain gauges are applied to all slabs. The top and bottom fibers of the slabs have external strain gauges adhered to their surface. Additionally, dial gauges are fastened to supports, one-third load locations, and the center.

In order to do support repairs, dial gauges are fixed at the supports. Demec gauges are also utilized to measure the linear stresses at the center and one-third load points. Brass pellets are affixed to the top, bottom, and center fibers at a predetermined distance in order to establish a standard gauge distance, which is necessary in order to measure strains with Demec gauges. In addition, LVDTs with a range of 0-100 mm are utilized to measure vertical deflections at one third locations and mid span. Up until the slabs collapse, the stress is supplied progressively in increments of 2 kN. A crack width detecting microscope is used to measure the crack widths on a regular basis. The experimental configuration is displayed in Fig. 1 and 2.

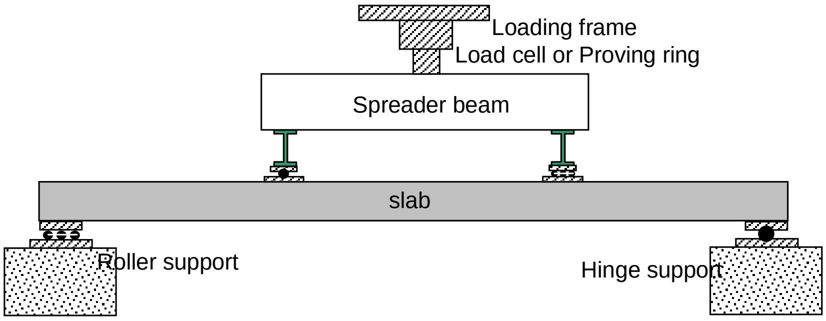

Fig.1 Experimental Test setup

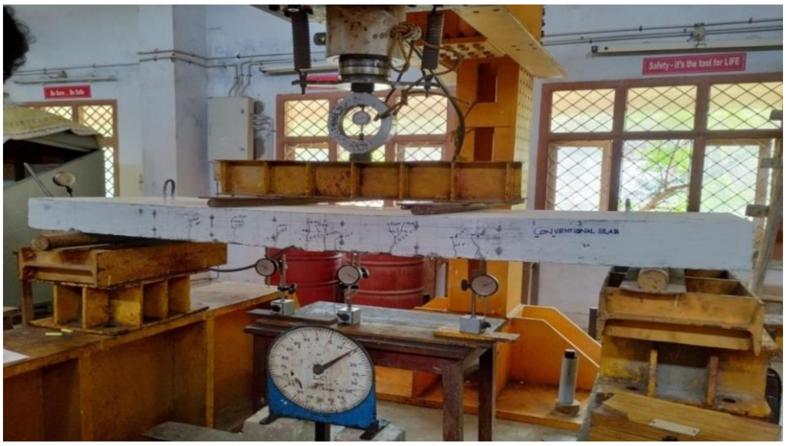

Fig.2 Photograph of Test Set up for Static loading

C. Experimental Results

The conclusions derived from this static loading test were based on testing 4 one way slabs cast with different parameters such as Compressive Strength, Rebar ratio, thickness of slabs (Table III).

Table.III Results of Flexural Investigation on Slabs

Sl No	Designation of slabs	P_{fc} (kN)	P_u (kN)	$M_{u,}$ kNm	w_{cr} Mm	ΔU mm	ε_c	ε_s
1	GG-M1R1D1	10	40	12	1.7	55	0.0007	0.005
2	GG-M1R2D1	12	47.5	14.25	1.5	54	0.0005	0.0039
3	GG-M1R1D2	15	54	16.2	1.5	39.2	0.0003	0.0036
4	GG-M2R1D1	18	47	14.1	1.2	39.2	0.0005	0.0029

V. FACTORS INFLUENCING FLEXURAL CAPACITY OF ONE WAY SLABS

Developing the resistance models for one way slabs require investigating a wide range of realistic parameters in the design space. In this study, one way slabs are designed according to Indian standards without considering the material partial safety factors. Two slab thicknesses, (100 mm and 120 mm), two concrete compressive strengths (M25 and M50 grades of concrete), two different GFRP reinforcement ratios (R1 and R2), are considered for reliability analysis. Totally 4 slabs are considered for reliability analysis.

In order to account for the randomness of variables influencing the flexural capacity of GFRP reinforced concrete one-way slabs, the current work used reliability-based approaches. The Monte Carlo simulation flowchart utilized for the reliability study is shown in Fig.3.

Three categories can be used to classify the potential sources of ambiguity regarding the resistance

- Material properties (M): uncertainties in the material's strength, modulus of elasticity, cracking stresses, etc. are all part of material properties.
- Fabrication (F): these are the unknowns in the member's overall dimensions that can impact the cross-sectional area, second moment of area, and other parameters.
- Analysis (P): the degree of uncertainty brought about by approximation techniques. Every one of these sources of uncertainty has unique statistical characteristics, such as distribution type, bias, and coefficient of variation.

Generally speaking, the resistance model's mean value can be written as:

$$\mu_R = M_n \mu_M \mu_F \mu_P \qquad (1)$$

where M_n is the member's nominal capacity and M, F, and P are their respective mean values.
As a result, the coefficient of variation and bias fact or that characterize the resistance model of are provi ded as $\lambda_R = \lambda_M \lambda_F \lambda_P$ (2)

$$V_R = \sqrt{{V_M}^2 + {V_F}^2 + {V_P}^2} \qquad (3)$$

Where $\lambda_M,\ \lambda_F\ and\ \lambda_P$ are the bias factors and V_M, V_F and V_p are the coefficients of variation of M, F and P respectively.

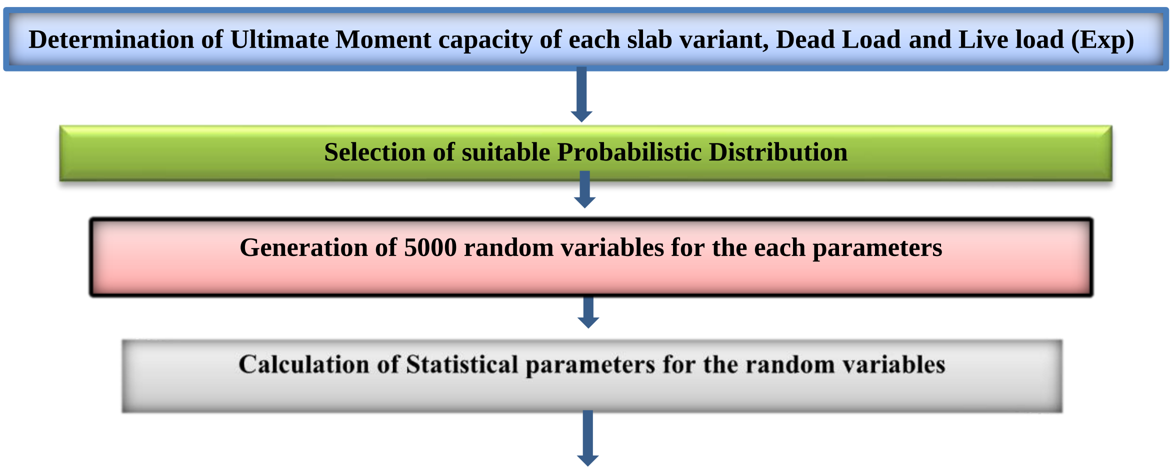

Fig.3.Flow chart of Monte carlo simulation procedure.

VI. STATISTICAL PROPERTIES

A. *Materials*

The statistical data pertaining to the compressive strength of concrete f_c and elastic modulus E_{GPC} are obtained from experimental studies and modelled as lognormal random variable. The statistics of tensile strength of reinforcements is obtained from manufacturers and is modelled as Normal distribution. To carry out the Montecarlo simulation for the materials Microsoft Excel Spreadsheet is used.

Table. IV Statistical properties of materials constituting slabs

Materials		Bias λ_M	COV %, V_M	Distribution
Compressive strength of GPC	M1	1.1	3	Normal
	M2	1.1	3	
Area of GFRP bars, A_{GFRP} mm^2		1.2	1.5	Normal

The statistical properties of materials constructing the slabs (taken from the literature [22]) and elastic modulus are shown in Table IV and Table V.

Table. V Statistical properties of the Elastic Modulus of GPC

Number of generated values for each specimen	Mean	Std Deviation	COV	Bias	Distribution
5000	25000	3	0.025%	1	Normal
5000	25225	3	0.025%	1	
5000	25250	3	0.025%	1	

B. *Dimensions of the slabs*

With regard to the properties of overall dimensions *b* (width of slabs) and D_1, D_2 (thickness of slabs), a normal distribution is adopted whose bias and COV are 1 and 3 respectively [16] - [18] and [22]. The statistical information are tabulated in Table VI.

Table. VI Statistical Properties of Slab Dimensions

Variable, mm		Bias(λ_F)	COV (%) (V_F)	Distribution
Width of Slab, b		1	3	Normal
Thickness of Slab	D_1	1	3	
	D_2	1	3	

C. *Tensile strength of the reinforcements*

Regarding the statistical properties of tensile strength of reinforcements, a large number of random parameters are involved. These include the various fibre volume proportions and testing methods. The statistical information on these parameters and their influence on the flexural behaviour of concrete slabs are very difficult to be ascertained. However, in the present study, the upper and lower bound values are obtained under extreme parametric conditions. With these, Monte Carlo Simulations are used to simulate the distribution type. Statistical properties of tensile strength of the steel / GFRP reinforcements are determined with the help of 'Histograms'. A histogram is a statistical information presentation that shows the frequency of data items in consecutive equal sized numerical intervals using rectangles. Plotting the independent variable along the horizontal axis and the dependent variable along the vertical axis is the most popular type of histogram. A process data set's distribution can be visually summarized and shown using a histogram. Histograms of tensile strength for GFRP reinforcements used in the present study are shown in Fig. 4.

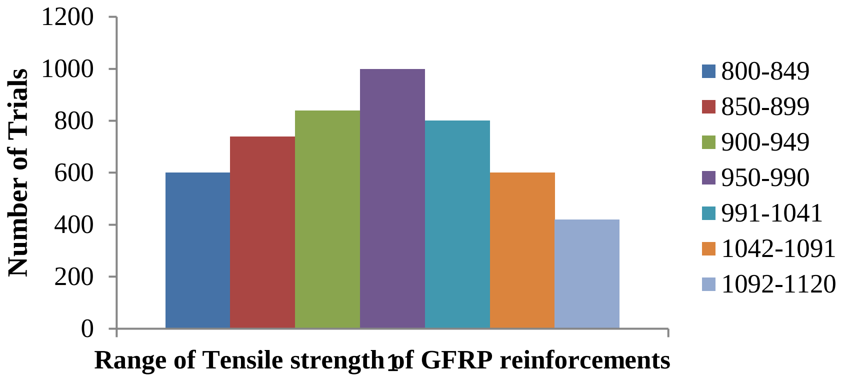

Fig. 4. Histogram showing the tensile strength of 10mm dia GFRP reinforcements

To find the best statistical representation, a variety of distribution types are examined. At a significance level of 5%, the Weibull distribution (Extreme Event Type III) describes the material properties of GFRP bars, according to a chisquare statistical test. An overview of the statistical characteristics of GFRP reinforcements employed in this study is provided in Table. VII.

Table. VII Statistical properties of tensile strength of steel/GFRP reinforcements

Type of bars (diameter, mm)	Tensile strength (MPa)		Bias (μ_M)	Std dev	COV (%) (V_M)	Type of Distribution
	Nominal (Exp)	Mean				
GFRP Rebar (10 mm),MPa	986	952	0.97	19.7	2%	Weibull

VII. THEORETICAL METHOD FOR GPC-GFRP REINFORCED ONE WAY SLABS

The accuracy of Theoretical Analysis method used in this study are verified by comparing flexural strengths obtained experimentally and analytically. The uncertainty in the analytical model is derived by means of a bias, and a coefficient of variation, V_P using Eqs. (4) and (5) and are tabulated in the Table. VIII.

$$\lambda_P = \mu\left(\frac{M_{exp}}{M_{Anal}}\right) \quad (4)$$

$$V_P = cov\left(\frac{M_{exp}}{M_{Anal}}\right) \quad (5)$$

Table. VIII Statistical properties for the uncertainities in Analysis

S.No	Designation of slabs	Ultimate Moment (kNm)		(b) / (a)
		Analytical method (a)	Experimental method (b)	
1	GG-M1R1D1	11.56	12.00	1.04
2	GG-M1R2D1	13.63	14.25	1.05
3	GG-M1R1D2	15.40	16.20	1.05
4	GG-M2R1D1	13.35	15.00	1.12
5	OS-M1R1D1	8.98	10.65	1.20
6	OG-M1R1D1	11.56	11.58	1.10
7	GS-M1R1D1	9.00	10.80	1.18
			Mean	1.10
			Std Dev	0.08
			COV	7.28 %

A. *Material and fabrication of one way slabs*

Five thousand randomly generated data sets for each type of slab are used to determine the mean and standard deviation of the moment capacities measured using the experimental approach .Fig.5 presents the distribution of 5000 Random Variables generated for the Ultimate Moment (Exp) for Slab GG-M1R1D1. For all the four slabs constructed in the present study, Monte Carlo simulations have been executed and the statistical properties have been determined and tabulated in Table. IX.

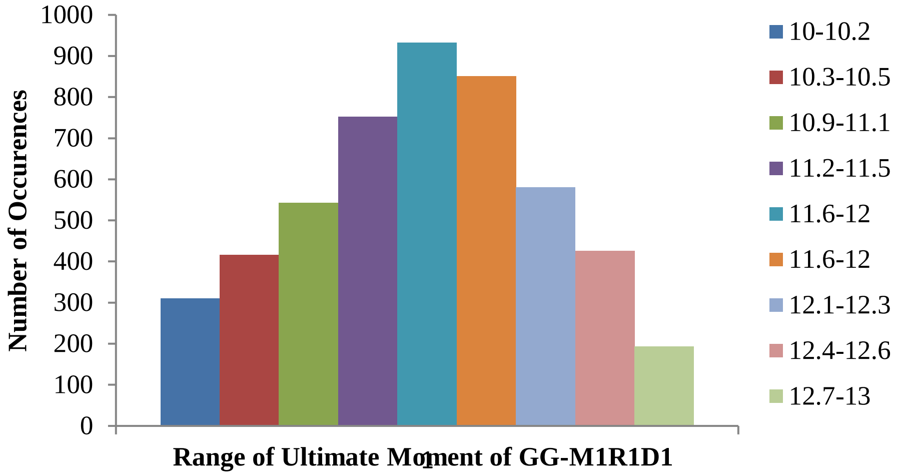

Fig.5. Distribution of Random Variables generated for the Slab GG-M1R1D1

Table. IX. λ_{MF} and V_{MF} of GFRP reinforced concrete one way slabs

Sl.No	Slab specification	Flexural capacity (kNm)			Bias (λ_{MF})	COV % (V_{MF})
		Nominal (Exp)	Mean (μ_{MF})	Std.Dev σ_{MF}		
1	GG-M1R1D1	12.00	11.82	1.18	0.99	17.30
2	GG-M1R2D1	14.25	13.82	1.31	0.97	18.60
3	GG-M1R1D2	16.20	15.55	1.44	0.96	19.50
4	GG-M2R1D1	15.00	13.25	1.20	0.90	18.42

A higher bias for slabs numbered 1 indicate that the failure of GFRP reinforced slabs is governed purely by GFRP rupture. On increasing the reinforcement ratio, thickness of slab and Concrete grade of slabs, the bias gets decreased and COV gets increased due to the increase in Moment capacity of slabs. Similarly, a lower COV is acquired for slab numbered 1. This may be due to the yielding nature of steel rebars.

VIII. LOADS

The statistical information about the load random variables used in general reliability studies is taken into consideration in this study and is shown in the Table. X. The structure's self-weight causes the dead load to be the gravity load taken into account during design, while the optimum live load is a load that is evenly distributed. The statistical characteristics of live load are significantly influenced by the place in question. As the area contributing to the live load increases the maximum load intensity for the 50-year design life—the magnitude of the load intensity falls. Based on Indian standards, statistical information on the dead and live load variables is taken from the literature for this study.

Table. X Statistical Properties for Dead and Live loads [22]

Types of Load	Bias	COV (%)	Distribution
Dead Load	1	10	Normal
Live Load	1	18	Extreme Event I

IX. RELIABILITY MODEL

The probability of failure P_f may be calculated as follows, assuming R and Q to be statistically independent (Fig,6).

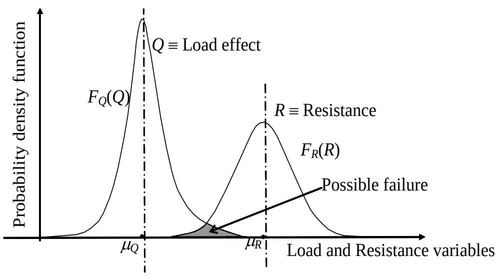

Fig. 6. Fundamental reliability model

$P_f = Prob\ [R < Q]$ (6)

$P_f = Prob[\{R < Q\} \cap \{0 < Q < \infty\}]$ (7)

$P_f = \int_0^{\infty} f_Q(Q) \left[\int_0^{Q} f_R(R) dR\right] dQ$ (8)

Alternatively, it defines the 'Margin of safety', Z as a random variable as follows:

$Z = R - Q$ (9)

The probability of failure may be conveniently expressed as

$P_f = Prob\ [Z < 0]$ (10)

If R and Q are assumed to be independent, normally distributed variables, Z will also have a normal distribution (with mean μ_M and standard deviation σ_M), and

$P_f = \Phi(-\beta)$ (11)

where Φ denotes the standard normal distribution function and $\beta \equiv \mu_M / \sigma_M$ is called the mean value-based "reliability index". In general, however, M will not be a normal distribution. Nevertheless, the relation between β and P_f given by Eqn (11) is frequently used and in such cases P_f is referred to as the "nominal probability of failure."

A. First Order Reliability Method (FORM)

In this study, FORM is used to assess the safety levels i.e evaluating the probability of failure P_f (or the reliability index,β) underlying a given structure. FORM derives its name from the fact that it is based on a first order Taylor series approximation of the limit state function. The linearization is done in the transformed z-space at the "design point" (shortest distance from origin), using the second moment statistics (mean and covariance) of the random variables. In FORM, the information on the distribution of random variables is ignored. The limit state functions under consideration are first formulated in the original co-ordinates (X_i). All variables are then transformed into uncorrelated standard normal variables and the limit state function is then transformed into the z_i co-ordinates. In the present problem, all the basic variables are uncorrelated, whereby

$$z_i^* = \frac{x_i - \mu_{X_i}}{\sigma_{X_i}} \quad (12)$$

The gradients with respect to the transformed co-ordinates are derived and used in the computation of the reliability index β and the failure point. An initial failure point is assumed (usually the mean values), and the reliability index β is estimated as the distance between the origin of the transformed co-ordinate space and the failure point. Successive failure points are calculated iteratively and a new value of β is found. In this study, the determination of reliability index is based on steps recommended by Nowak and Collins (2000). This procedure transforms the basic variables X into equivalent normal and uncorrelated variables U (Fig. 7 (a), (b) and (c)).

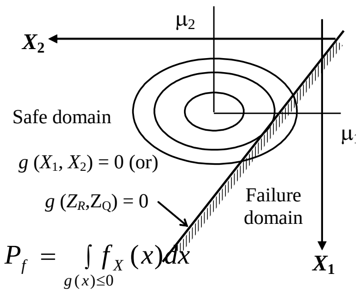

Fig.7(a): Original co-ordinates

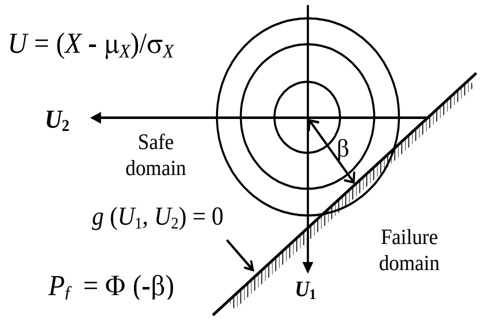

Fig.7(b): Transformed co-ordinates

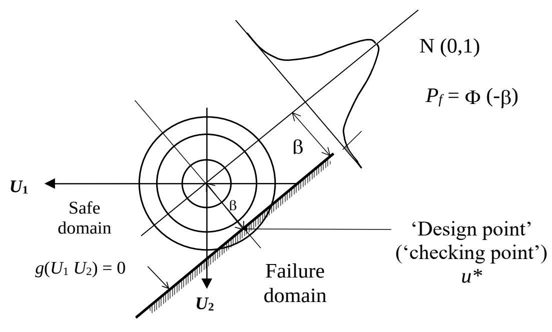

Fig. 7(c): Reliability index

The term β is defined as the minimum distance from the origin of the design space to the failure hyper surface U.

$$\beta = \min_{U \in \{g(U)=0\}} \sqrt{\sum_{i=1}^{n} u^{*2}_{i}} \quad (13)$$

In the present study, random variables will first be normalized by transforming them into their standard forms, which is a non dimensional form of a variable. For the simple limit state function in Eqn.(14), the standard forms of the basic variables R and Q can be expressed as

$$z_R = \frac{R-\mu_R}{\sigma_R} \text{ and } z_Q = \frac{Q-\mu_Q}{\sigma_Q} \quad (14)$$

where, Z_R and Z_Q are called reduced variables and μ_R and μ_Q are the means, and $\sigma_R$and σ_Q are standard deviations for variables R and Q, respectively. The limit state function,

$$g(Z_{R,} Z_Q) = (\mu_R - \mu_Q) + z_R\sigma_R - z_Q\sigma_Q \quad (15)$$

For any specific value of g (z_R, z_Q), Eqn. (15) represents a straight line in the space of reduced variables z_R and z_Q. The line g (z_R, z_Q) =0 separates the safe and failure zones in the space of reduced variables. The reliability index,β is defined [18] as the shortest distance from the origin of the reduced variables to the line g(z_R, z_Q) = 0. FORM is utilized to get the shortest distance. The foundation of FORM is a first order Taylor Series expansion of the limit state function, which uses a tangent plane at the point of interest to simulate the failure surface. A nonlinear limit state function or a function with more than two random variables may not necessarily have a closed form solution. Therefore, the Taylor series Eqn.(16) is utilized to transform a non-linear limit state function into simple polynomials.

The expansion of a function, f (X) at a certain point "a" is given by;

$$f(X) = f(a) + (X-a)f'(a) + \frac{(X-a)^2}{2}f''(a) + \ldots\ldots\ldots\ldots \frac{(X-a)^n}{n!}f^n(a) \quad (16)$$

By taking into account the Taylor series expansion after truncating all terms of higher order except the first order terms, FORM employs this expansion to simplify the limit state function, [g(z1, z2… zn)]. At the actual design point X*, the expansion is carried out. An iterative procedure is required to find this point in the design space, g (z1, z2… zn) = 0 (Nowak and Collins 2000). Iteratively solving a set of (2n+1) simultaneous equations with (2n+1) unknowns is necessary for the convergence of a design point, where

$$\alpha_i = \frac{-\frac{\partial g}{\partial z_i}\Big|_{evaluatedatdesignpoint}}{\sqrt{\sum_{k=1}^{n}\left(\frac{\partial g}{\partial z_i}\Big|_{evaluatedatdesignpoint}\right)^2}} \quad (17)$$

$$\frac{\partial g}{\partial z_i} = \frac{\partial g}{\partial X_i}\frac{\partial X_i}{\partial z_i} = \frac{\partial g}{\partial X_i}\sigma x_i \quad (18)$$

$$\sum_{i=1}^{n}(\alpha_i)^2 = 1 \quad (19)$$

$$z_i^* = \beta\alpha_i \quad (20)$$

$$g(z_1^*, z_2^*, \ldots, z_n^*) = 0 \quad (21)$$

where $z_i^*$is the design point in converted space and α_i is a unit vector pointing from the origin toward a design point. The necessity that the design point be on the failure boundary is expressed mathematically and the underlying premise of this process is that the random variables involved are regularly distributed. It is necessary to determine the equivalent normal values of the mean and standard deviation for each nonnormal random variable when the probability distributions for the variables involved in the limit state function are not normally distributed. The CDF and PDF of the real function should equal the normal CDF and normal PDF at the value of the variable X * on the failure boundary described by g=0 in order to achieve the equivalent normal mean and standard deviation.

Mathematically it can be expressed as

$$F_X(X^*) = \Phi_1\left(\frac{X^*-\mu_X^e}{\sigma_X^e}\right) \quad (22)$$

$$f_X(X^*) = \frac{1}{\sigma_X^e}\Phi_2\left(\frac{X^*-\mu_X^e}{\sigma_X^e}\right) \quad (23)$$

Where, X is a random variable with mean $\mu_X$and standard deviation $\sigma_X$and is described by a CDF $F_X(X)$ and a PDF $f_X(X)$. $\Phi_1(X)$is the CDF for the standard normal distribution and $\Phi_2(X)$is the PDF for the standard normal distribution. Expressions for μ_X^e and σ_X^e can be obtained as follows:

$$\mu_X^e = X^* - \sigma_X^e[\Phi^{-1}(F_X(X^*))] \quad (24)$$

$$\sigma_X^e = \frac{1}{f_X(X^*)}\Phi_2\left[\Phi^{-1}\left(F_X(X^*)\right)\right] \quad (25)$$

The basic steps in the iteration procedure (Nowak and Collins 2000) to obtain reliability index are as follows:

1. Formulate the limit state function. Determine the probability distributions and appropriate parameters for all random variables X_i (i =1, 2 …, n) involved.

2. Obtain an initial design point $\{X_i^*\}$ by assuming values for n-1 of the random variable. (mean values are a reasonable choice.) Solve the limit state equation g=0 for the remaining random variable which ensures that the design point is on the failure boundary.

3. Equivalent normal mean, and standard deviation, μ_X^e, σ_X^e are determined using Eqns (24) and (25) for design values corresponding to a non normal distribution.

4. Determine the reduced variables $\{z_i^*\}$ corresponding to the design point $\{X_i^*\}$ using

$$z_i^* = \frac{X_i^* - \mu_{Xi}^e}{\sigma_{Xi}^e} \qquad (26)$$

5. Determine the partial derivatives of the limit state function with respect to the reduced variables. {G} is a column vector whose elements are the partial derivatives multiplied by -1.

$$\{G\} = \begin{Bmatrix} G_1 \\ G_2 \\ . \\ . \\ G_n \end{Bmatrix}$$

$$where,\ G_i = -\frac{\partial g}{\partial z_i}\bigg|_{evaluated\ at\ design\ point} \qquad (27)$$

6. Estimation of β is then calculated using the following formula.

$$\beta = \frac{\{G\}^T\{z^*\}}{\sqrt{\{G\}^T\{G\}}}$$

$$where,\ \{z^*\} = \begin{Bmatrix} z_1{}^* \\ z_2{}^* \\ . \\ . \\ z_n^* \end{Bmatrix} \qquad (28)$$

7. The direction cosines for the design point to be used in the subsequent iteration are then calculated using

$$\{\alpha\} = \frac{\{G\}}{\sqrt{\{G\}^T\{G\}}} \qquad (29)$$

8. Determine a new design point for n-1 of the variables using

$$z_i^* = \alpha_i \beta \qquad (30)$$

9. Determine the corresponding design point values in original coordinates for the n-1 values in Step 7 by

$$X_i^* = \mu_{Xi}^e + z_i^* \sigma_{Xi}^e \qquad (31)$$

10. Determine the value of the remaining random variable by solving the limit state function g = 0

11. Repeat Steps 3 to 10 until β andX_i^*converge. A simple Microsoft Excel Spread sheet is used to carry out the above procedure.

B. Reliability Based Design

For a given failure criterion, reliability-based design makes sure the structural risk acceptance criteria match the target reliability, which is the necessary minimum reliability. The results of a reliability-based design should ultimately be converted into safety factors, such as the resistance factor used in this investigation. However, it is typically advised that when creating a new code specification, the "β" values that highlight current practice should be identified first, and then the target β should be selected to roughly correspond to an acceptable range of values acquired. The desired reliability is also determined by socioeconomic factors. Setting such goal reliability has the practical benefit of ensuring consistency in safety and economics for the corresponding reliability-based design [22]. It should be mentioned, nonetheless, that the code calibration authorities have the final say over the desired reliability. The Load and Resistance Factor Design (LRFD) format, which is used in this study, is arguably the easiest to comprehend of the numerous safety factor formats currently in use. When applying the LRFD idea to the conventional dependability model, the following prerequisite must be met in order for there to be adequate safety.

Design Resistance $(\phi\ R_n) \geq$ Design Load effect $(\gamma\ Q_n)$ (32)

The resistance factor is less than unity because it takes into consideration under strength, or a potential deficiency in the calculated "nominal" resistance, due to uncertainties pertaining to material strengths, dimensions, theoretical assumptions, etc. The evaluation of the resistance factor for the suggested design of one-way slabs made of GFRP reinforced concrete is the main focus of this work. The literature has provided the statistical parameters associated with load modelling [16]-[18].The limit state functions must be developed in order to assess the dependability index for the GFRP reinforced concrete one-way slabs.

It consists of three random variables, flexural resistance M_R, applied bending moment due to Dead Load (DL) effect, M_D and applied bending moment due to Live Load effects, M_L

$$g(M_R, M_D, M_L) = M_R - (M_D + M_L) \qquad (33)$$

The load demands M_D and M_L are obtained by back-calculating from the design equation. By assuming a certain LL to DL effect ratio, the load demand can be quantified. For example, in the case of equal LL and DL effect, the design equation is given by

$$\gamma_D M_D + \gamma_L M_L = \phi\, M_n \qquad (34)$$

Eqn. (34) can be used to calculate M_n, M_D, M_L. The ratio of LL to DL is taken as one in this study. Table. XI lists the reliability indices, or β, that were computed for one-way slabs of GFRP reinforced concrete for the ratio. According to the study, when the reinforcement ratio rises from 0.65% to 1.15 percent, the reliability index falls from 0.82 to 1.15 %. In a similar vein, as slab depth and concrete strength increase, the reliability index falls. All of the parameters taken into consideration in this study had their β values computed and summarized in Table. XI. According to the study, reliability index values fall between 3.5 and 4.1, that is conservative in comparison to the design of conventionally reinforced concrete slabs. Additionally, it has been noted that the dependability of GFRP reinforced slabs is impacted by the concrete's compressive strength. In conclusion, as long as strength and serviceability requirements are met, both failure modes—that is, FRP rupture and concrete crushing—are permissible for the design of flexural members reinforced with GFRP reinforcements. The recommended margin of safety against failure is consequently greater than that employed in conventional steel reinforced concrete section design in order to make up for the lack of ductility. The probabilistic equation is $\emptyset = 1 - 0.75\beta Vg$ where Vg is the coefficient of variation and β is the Reliability or dependability index used to calculate the resistance factor. Table. XII displays the values for the various slab parameters that have been calculated and compared to the current design standards. Eqns. (1) to (34) are used to determine the Reliability Index and Resistance Factor of GPC – GFRP One way slabs in the present study.

Table. XI Reliability Index, (β) and Resistance factors of all slabs (Present study)

Sl.No	Slab Designation	β ($M_L/M_D = 1$)	COV $V_{g,\%}$	Resistance factor,∅
1	GG-M1R1D1	4.10	17.30	0.65
2	GG-M1R2D1	3.50	18.60	0.67
3	GG-M1R1D2	3.91	19.50	0.61
4	GG-M2R1D1	3.93	18.42	0.60

Table. XII. A comparison with previous authors and present study

S.No	Previous studies	Reliability Index	Resistance factor ∅
1	ACI 440-1R (CC - GFRP)		0.75
2	JSCE,1997 (CC - GFRP)		0.77
3	Sivagamasundari and Kumaran,2012 (CC - GFRP)	4.13	0.74
4	Current Study, 2024 (GPC - GFRP)	3.91 - 4.10	0.60 to 0.65 (Tension controlled)
5	Current Study, 2024 (GPC - GFRP)	3.50	0.67 (Compression Controlled)

X. DISCUSSION OF RESULTS

Probability is important for structuring the conceptual framework of the uncertainty analysis. The resistance factors are calibrated using the Experimental (Present Study) database. The target reliability indices for limit states of strength involving dead and live loads are typically regarded as 3.0 or 3.5, according to the literature that is currently accessible. The investigation mentioned above leads to the following observations.

- To meet the calculated β, $\emptyset$ value for all seven slabs have been determined and is found to be between 0.6 - 0.70.

- It was discovered that the calibrated $\emptyset$ satisfied the safety requirements set forth by the design code while producing a more cost-effective and less conservative design.

- For tension controlled slabs the resistance factor is 0.6 to 0.65 and for compression controlled slabs the resistance factor is 0.67.

- When the reinforcement ratio rises from 0.49 to 0.52 the reliability index falls by 15%. The primary cause of this is the increased likelihood of an early brittle failure at high reinforcing ratios.

- A higher reliability index is recommended for GFRP reinforcement ratios equal to or less than one in order to prevent the GFRP rupture mode of failure. When comparing M50 grade GFRP reinforced concrete one-way slabs to M25 grade GFRP reinforced concrete one-way slabs, the reliability index is lower (4.15%). The reliability index is influenced by the concrete's compressive strength. This could be because the slab's ductile nature may be reduced when its strength increases due to an increase in compressive strength.

- On increasing the thickness of one-way slabs, β decreases by 4.6% showing that the higher reserve capacity of slabs needs a lesser reduction factor.

- The reliability study is carried out for the live load to dead load ratio of one i.e., M_L/M_D =1.

- The cross-sectional properties of the GFRP slabs such as the member width and thickness has no major influence on the reliability index.

XI. CONCLUSIONS

The current study's findings show that depending on the anticipated mechanism of failure, GFRP reinforced concrete one way slabs have different statistical characteristics. Higher reinforcement ratio slabs fail due to concrete crushing, so the statistical characteristics of the concrete have a greater impact on the resistance models. Different resistance models that are impacted by the rupture of GFRP reinforcements are imparted by a lower reinforcement ratio. In reliability-based design, this information is crucial since it affects design parameters like the resistance factor. Slabs that fail due to GFRP bar rupture have larger bias values than slabs that fail due to concrete crushing. The fact that the GFRP rupture mode produces a lower coefficient of variation balances these bias values.

REFERENCES

[1] AASHTO, (2014),- AASHTO LRFD Bridge Design Specifications, *7th Edition, American Association of State Highway and Transportation Officials, Washington, D.C*.

[2] ACI Committee 440, 2001,- Guide for the design and construction of concrete reinforced with FRP bars, *ACI 440.01R-05, American Concrete Institute, Farmington Hills, Mitch*.

[3] Aiello M., and Ombres L.,- Load-Deflection Analysis of FRP Reinforced Concrete Flexural Members, *Journal of Composites for Construction*, Vol.4, No.4, November, 2000.

[4] Amy K., - *Design Methods for FRP-Strengthened Concrete using Sheets or Near-Surface Mounted Bars, University of Manitoba*, March 28, 2002

[5] Atadero R., Lee L., and Kambhari V.,- Materials Variability and Reliability of FRP Rehabilitation of Concerete, *Proceedings of the 4th International Conference on Advanced Composite Materials in Bridges and Structures*, *ACMBS IV, Canada*, July 2004.

[6] Caltrans, (2014).- *California Amendments to AASHTO LRFD Bridge Design Specifications – 6th Edition, California Department of Transportation, Sacramento, CA*.

[7] CSA, (1998).- *Canadian Highway Bridge Design Code, Canadian Standards Association, Rexdale, Ontario, Canada*.

[8] Desayi P , Rao K B . Markov,- Chain Model for Cracking Behavior of Reinforced Concrete Beams. *Journal of Structural Engineering*, 1989, 115(9):2129-2144.

[9] Ellingwood, B.E., MacGregor, J.G., Galambos, T.V., and Cornell, C.A. (1982).- "Probability-Based Load Criteria: Load Factors and Load Combinations," *Journal of Structural Division, ASCE*, 108(5), 1337-1353.

[10] Faber M., and Sorensen J.,- *Reliability Code Calibration, Paper for the Joint Committee on Structural Safety Draft*, March 2002.

[11] Ferreira A., Camanho P., - Marques A., and Fernandes A., Modelling of Concrete Beams Reinforced with FRP Rebars, *Composite Structures*, Vol. 53, 2001

[12] Galambos, T.; Ellingwood, B., - MacGregor, J.; Cornell, C,- Probability Based Load Criteria: Assessment of Current Design Practice. *J. Struct. Div*. 1982, 108, 959–977. [Google Scholar] [CrossRef]

[13] GB 50068-2018; - *Unified Standard for Reliability Design of Building Structures. China Building Industry Press: Beijing, China*, 2019. (In Chinese)

[14] Lu, R.; Luo, Y.;- Conte, J.P. Reliability Evaluation of Reinforced Concrete Beams. *Struct. Saf.* 1994, 14, 277–298. [Google Scholar] [CrossRef]

[15] Nasrollahzadeh K , Aghamohammadi R, -Reliability analysis of shear strength provisions for FRP-reinforced concrete beams, *Engineering Structures*, 2018, 176:785-800.

[16] Nowak, A.S. (1993)., - "Calibration of LRFD Bridge Design Code, *Department of Civil and Environmental Engineering Report UMCE 92-25, University of Michigan, Ann Arbor, MI*.

[17] Okeil M. Ayman., and Sujata Kulkarni (2006)., - Flexural Resistance Models for Concrete Decks Reinforced with FRP Bars, *TRB 2006 Annual Meeting* CD-ROM 1 – 16.

[18] Ranganathan.R.(1999).,-*Structural Reliability Analysis and Design, Jaico Publishing House, NewDelhi*

[19] Ravindra, M.K., and Galambos, T.V. (1978),- Load and Resistance Factor Design for Steel, *Journal of Structural Division, ASCE*, 104(ST9), 1337-1353.

[20] Sergey A. Solovyev, Anastasia A. Solovyeva1 , Alexander A. Kochkin , Timur R. Akhmetov, -Reliability analysis of the existing reinforced concrete beams with normal cracks by rebar strength criteria, *E3S Web of Conferences 220*, 01043 (2020) https://doi.org/10.1051/e3sconf/202022001043 SES-2020

[21] Simwanda L , Koker N D , Viljoen C,- Structural reliability of ultra high-performance fibre reinforced concrete beams in flexure, *Engineering Structures*, 2021, 244:112767.

[22] Sivagamasundari.R and Kumaran G,(2012) ,- Reliability analysis of concrete Oneway slabs reinforced internally with GFRP Reinforcements under Repeated Loading, *ICFAI university journal of structural Engineering*, Vol.V(2), Apr 2012, pp. 7-27. 2012.

[23] Vincent, G.S. (1969).- Tentative Criteria for Load Factor Design of Steel Highway Bridges, *AISI Bulletin 15, American Iron and Steel Institute, Washington, DC*

[24] Xiea.H, Y. Wanga., R. Zoub.- Reliability analysis of RC T-beam highway bridges in China based on a virtual bridge dataset. *Eng. Struct.*, 104 (2015).

[25] Yan, BaoqiHui, YueMohamed, Hamdy,- Reliability analysis of concrete beams based on the stochastic model of resistance calculation, *Applied Mathematics and Nonlinear Sciences*, Vol.8 (1) 2023.

[26] Zhou, Y.; Zhang, J.; Li, W.; Hu, B.; Huang, X,- Reliability-Based Design Analysis of FRP Shear Strengthened Reinforced Concrete Beams Considering Different FRP Configurations. *Compos. Struct.* 2020, 237, 111957. [Google Scholar] [CrossRef]

[27] Zhang, W.; Liu, X.; Huang, Y,- Tong, M.-N. Reliability-Based Analysis of the Flexural Strength of Concrete Beams Reinforced with Hybrid BFRP and Steel Rebars. *Archiv. Civ. Mech. Eng*. 2022, 22, 171. [Google Scholar] [CrossRef]